ELSEVIER

Chemical Engineering Journal 130 (2007) 87–99

Chemical Engineering Journal

www.elsevier.com/locate/cej

Estimation of particulate velocity components in pneumatic transport using pixel based correlation with dual plane ECT

Urmila Datta [a], Tomasz Dyakowski [b], Saba Mylvaganam [a,c,*]

[a] *Tel-Tek, Kjølnes Ring, N-3918 Porsgrunn, Norway*

[b] *Department of Chemical Engineering, P.O. Box 88, Manchester M60 1QD, UK*

[c] *Telemark University College, Faculty of Technology, Kjølnes Ring 56, N-3914 Porsgrunn, Norway*

Abstract

This article presents a technique developed to estimate the velocity components of two phase solid/gas flow using electrical capacitance tomography (ECT). The pixel by pixel correlation method for consecutive frames in a given sensor plane has been used to trace the particle velocity profile in the transverse direction. The transverse movement of solid particles in slug flows has been reported recently in the literature. The transverse velocity of the particles is probably caused by the picking up mechanism experienced by single particles, to form a slug body. Rest of the particles following the slug forms a stationary layer thus exhibiting no transverse component. These phenomena have also been observed in earlier studies using high-speed video camera. The pixel-based correlation using ECT confirms these observations and also helps to detect the slugging phenomena. The same technique is implemented to trace the path of rotational motion of an object inside the sensor plane and also to detect the transverse motion of particulates in dilute phase vertical pneumatic conveying system. Both axial and transverse velocity components estimated by ECT are verified using Laser Doppler Anemometer (LDA).

Keywords: Pixel by pixel correlation; Slug flow; Transverse velocity; Dilute phase pneumatic transport; Electrical capacitance tomography

1. Introduction

The transport phenomena associated with pneumatic conveying of solid/gas are rather complex due to particle–particle, particle–gas and particle–pipe interactions. It is very difficult to isolate the effect of any one of these interactions in a given pneumatic transport system and to predict its performance. In order to design a cost efficient pneumatic transport system, it is important to estimate the effect of various parameters like velocity, material distribution, size of particulates, etc. on the transport capacity and pressure drop. It is an important design criterion to keep the pressure drop as low as possible. However, in pneumatic transport, wide pressure fluctuations are very common. The transport capacity of a pneumatic system is measured using transport rate averaged over time. Hence, an estimation of solid velocity, concentration, and consequently the mass flow rate in real time in a pneumatic transport system is quite useful. Process tomography, in particular dual plane tomographic system can be used to visualize the flow patterns. Information regarding flow phenomena can be determined from tomographs by estimating or measuring parameters such as concentration, mass flow rate, velocity distribution etc. along the direction of flow. The technique of measuring velocity field by cross-correlating pixel by pixel basis was described earlier [1,2] and successfully implemented in many applications. In tomography this correlation technique is used to obtain the particulate motion in axial direction. The cross-correlation is normally done using the concept of point-wise pair of sensor planes assuming only axial particulate motion. In practice, particulates may have motion in all possible directions. A new concept of best-correlated pair of pixels is used by Mosorov et al. [3] to overcome the basic assumption that flow pattern is frozen between the sensor planes. This concept is important for dynamic and turbulent nature of flow where the solid trajectory is unknown. The best correlated pixel method is modified further by Zhang et al. [4] to describe the characteristics of dispersed flow, eroding dunes with down flow and ring flow regime in an inclined plane introducing an additional term as 'transverse motion ratio'. The 'transverse motion ratio' is a parameter, which calculates the deviation of the solid trajectory from axial direction based on the best correlated pixel pair

* Corresponding author at: Telemark University College, Faculty of Technology, Kjølnes Ring 56, N-3914 Porsgrunn, Norway. Tel.: +47 35575151; fax: +47 35575250.

E-mail addresses: tom.dyakowski@umist.ac.uk (T. Dyakowski), Saba.Mylvaganam@hit.no (S. Mylvaganam).

1385-8947/$ – see front matter © 2006 Elsevier B.V. All rights reserved.
doi:10.1016/j.cej.2006.08.034

Nomenclature

A_1, A_2	cross-sectional area at two different positions of the transport pipe
B	neighborhood of n, m
$C_{k[n,m]}$	concentration of pixel coordinate n, m of kth frame
$C_{k+1[i,j]}$	concentration of pixel coordinate i, j of $k+1$th frame
$C_{Z_1[n,m]}$	concentration of pixel coordinate n, m of Z_1 plane
C_{Z_1q}	concentration of qth pixel in Z_1 plane
C_{Z_2q}	concentration of qth pixel in Z_2 plane
$C_{Z_2[n-\Delta n,m-\Delta m]}$	concentration of pixel coordinate $n-\Delta n, m-\Delta m$
E	number of electrodes
f_D	Doppler frequency shift
k	image number or frame number
L	separation between the two planes
M	number of capacitance measurements
n, m and i, j	pixel coordinates
N	total number of images
p	shift in time sequence frame number
P	pressure
P_1, P_2	pressures at two different positions of the transport pipe
r_i	radius of the motion of the object at ith pixel position
$R_{k(n,m],k+1[i,j]}$	cross-correlation function for pixel coordinates n, m of kth frame and i, j coordinate of $k+1$th frame
$R_{S_{Z_1},S_{Z_2}}$	cross-correlation function for the two signals $S_{Z_1}(t)$ and $S_{Z_2}(t)$
R_{Z_1q,Z_2q}	cross-correlation function for qth pixel in Z_1 plane and qth pixel in Z_2 plane
$R_{Z_1[n,m],Z_2[n-\Delta n,m-\Delta m]}$	cross-correlation function for pixel coordinate n, m in Z_1 plane and pixel coordinate $n-\Delta n, m-\Delta m$ in Z_2 plane
$S_{Z_1}(t)$	signal detected in Z_1 plane
$S_{Z_2}(t)$	signal detected in Z_2 plane
T	observation time
u_s	axial solid velocity
u_{slip}	slip velocity
u_t	transverse solid velocity
u_x	x-component of transverse velocity
u_y	y-component of transverse velocity
U	particle velocity measured by LDA
v_g	air velocity in empty tube
v_i	tangential velocity at ith pixel position
v_1, v_2	air velocities at two different positions of the transport pipe
V	volumetric flow rate

Greek letters

ε	voidage
θ	intersection angle between two coherent laser beams
λ	wavelength of laser beam
τ	time delay
τ_{max}	time delay corresponding to maximum of cross-correlation function
ω_i	angular velocity at ith pixel position

method. The radial velocity component is also measured and compared with computational fluid dynamics (CFD) simulation result in a radial flow fixed bed reactor [5] using electrical resistance tomography. The radial velocity component is obtained by correlating a group of pixels between consecutive frames within the plane.

There are well established methods [6] for measuring two-dimensional cross-sectional velocity field by particle image velocimetry (PIV), particle tracking velocimetry (PTV) and also by other imaging techniques like LDA. The main objective of this paper is to describe a technique to estimate the transverse component of velocity by correlating the successive reconstructed images of any sensor plane using ECT and also to validate the use of dual plane electrical capacitance tomography for solid velocity measurements in solid/gas phase.

2. Velocity profile using ECT

2.1. Correlation function

One frequently used method of flow measurement is based on estimation of cross-correlation function using two sets of data from sensors spaced axially apart along the flow stream. If $S_{Z_1}(t)$ and $S_{Z_2}(t)$ are the signals detected from the sensor planes Z_1 and Z_2 at instant t respectively, then the typical cross-correlation function is defined by the following equation [7]:

$$R_{S_{Z_1},S_{Z_2}} = \lim_{T\to\infty}\frac{1}{T}\int_0^T S_{Z_1}(t)S_{Z_2}(t+\tau)\,dt \quad (1)$$

where τ is the time delay between the two signals and T is the observation time. The time delay τ_{max} corresponding to the maximum value of cross-correlation function gives the transit-time of the flow between the two sensors. Using transit-time and distance L between two sensor planes, the axial solid velocity can be evaluated as:

$$u_s = \frac{L}{\tau_{max}} \quad (2)$$

This technique is used in dual plane ECT system for measuring solid velocity as shown in Fig. 1.

The raw signals can be directly used in cross-correlation algorithm to estimate solid propagation velocity [8]. It gives the estimate of averaged velocity over the cross-section but by correlating pixel by pixel from reconstructed image we get the velocity profile which is often more useful in practical applications.

For reconstructed images the cross-correlation function can be written as [9].

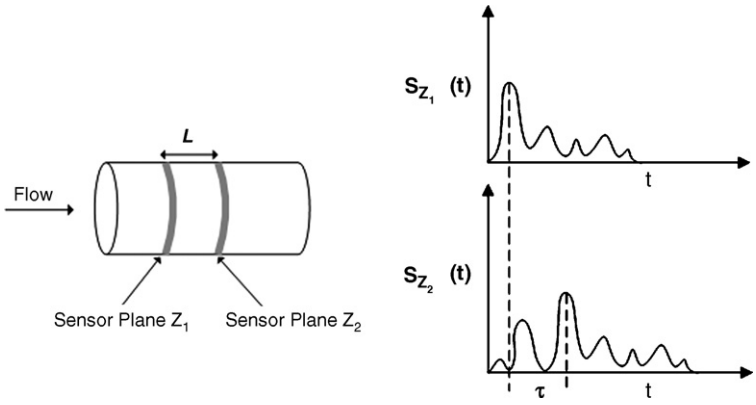

Fig. 1. Dual plane tomography system for velocity measurement using cross-correlation function. $S_{Z_1}(t)$ and $S_{Z_2}(t)$ are the signals detected from the sensor planes Z_1 and Z_2 at instant t, respectively.

$$R_{Z_1q,Z_2q} = \sum_{k=0}^{N-1} C_{Z_1q}[k]C_{Z_2q}[k+p] \tag{3}$$

where p is the shift in time sequence frame number, q stands for pixel index and N is the number of images in time-window.$C_{Z_1q}[k]$, $C_{Z_2q}[k+p]$ are the concentrations of pixel q of the image k of the sensor plane Z_1 and pixel q of the image $k+p$ of the sensor plane Z_2, respectively. This frozen model is a limitation because most solid/gas flow patterns are turbulent due to random movement of solids in gas. So in order to locate the solid trajectory and to estimate the resultant velocity Mosorov et al. [3] modified the correlation function as:

$$R_{Z_1[n,m],Z_2[n-\Delta n,m-\Delta m]} = \sum_{k=0}^{N-1} C_{Z_1[n,m]}[k]C_{Z_2[n-\Delta n,m-\Delta m]}[k+p], \quad (\Delta n, \Delta m) \in B \tag{4}$$

where the concentration of plane Z_1 at coordinate (n, m) is $C_{Z_1[n,m]}$ and $C_{Z_2[n-\Delta n,m-\Delta m]}$ is the pixel concentration at coordinate $(n-\Delta n, m-\Delta m)$ of the plane Z_2. B is the neighborhood of pixel coordinate (n, m) in plane Z_2.

2.2. A new approach of velocity estimated method

Axial component of solid velocity is estimated using classical method as direct cross-correlation function. An attempt is made here to develop a technique to estimate the transverse component by correlating consecutive frames in the same plane. For estimating transverse velocity components, the pixels are first grouped to form interrogation windows. The spatial resolution of the transverse velocity field is related to window size. The size of the window can be determined from the maximum value of the velocity component in transverse direction and the particle concentration. The window size is taken as 4×4 format in this study. Overlapping of the windows up to 50% is also considered. The concentration values of all the pixels for each interrogation window of one particular frame are correlated with all the pixel values of the next consecutive frame in the same sensor plane and the maximum of the correlation function is found with a resolution of one pixel for rough estimation. Sub pixel accuracy is then used to calculate the peak location using three point Gaussian curve fit method. The projected distance between two spatial coordinates in consecutive frames when divided by time interval between frames gives the transverse velocity components in sensor plane for these two consecutive frames. The velocity vectors are then located at the centre point of the window. The average velocity is computed using over an ensemble of 1000 image pairs.

Fig. 2 shows the technique used. The algorithm for calculating the correlation coefficient is [10]:

$$R_{k[n,m],k+1[i,j]} = C_{k[n,m]} \times C_{k+1[i,j]} \tag{5}$$

where k is the frame number, $C_{k[n,m]}$ the pixel concentration for coordinate (n, m) in kth frame and $C_{k+1[i,j]}$ is the pixel concentration for coordinate (i, j) of $(k+1)$th frame. The criterion for choosing the pixel pair is $\max\{R_{k[n,m],k+1[i,j]}\}$.

The chosen (n, m) and (i, j) are the pixel pairs in two consecutive frames k and $k+1$. If the projected distance between the chosen pixels pair (n, m) and (i, j) is d and the time delay between two consecutive frames is Δt, then the transverse velocity component is given by:

$$u_t = \frac{d}{\Delta t} \tag{6}$$

and

$$u_t = \sqrt{u_x^2 + u_y^2} \tag{7}$$

where u_x and u_y are x and y components of transverse velocity respectively. The time averaged velocity can be obtained using the three different methods as described in [11,12]. The three different methods are average velocity, average image and average correlation method. Here the average velocity method is adapted following certain steps like: (1) correlating two consecutive images such as image A_1 and image B_1, (2) detecting peak of instantaneous correlation, (3) calculating instantaneous velocity based on spatial coordinate shift and (4) finally averaging the velocity over a period of time. Fig. 3 shows the graphical representation of the method. This method can be used if the primary interest is to estimate instantaneous velocity in addition to average velocity measurement.

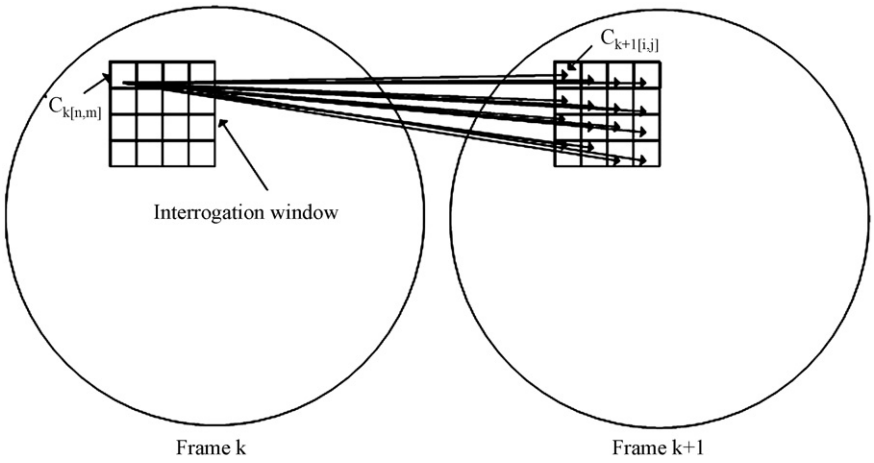

Fig. 2. Pixel by pixel correlation between two consecutive frames.

3. Components of the sensor suite used

3.1. Introduction

The sensor suites used for experimental purpose are described in brief in this section. A dual plane 8 electrode capacitance sensor system (PTL300) and a twin plane 12 electrode ECT system (PTL300E) with fixed sensor plane separation are used in experimental rig at the Department of Chemical Engineering, University of Manchester and in dilute phase vertical conveying rig at Telemark University College, Norway respectively. LDA system and X-Stream^{TM} VISION high speed CMOS digital camera is also used in same vertical rig.

3.2. Twin plane electrical capacitance tomography system

Electrical capacitance tomography exploits non-intrusively, spatial and temporal permittivity variations of the components leading to measurement of electrical capacitance between the set of electrodes mounted at the periphery of the process vessel. The number of measurements M possible for E electrode system is given by $M = E(E-1)/2$. The capacitive measurements are then converted into an image showing the distribution of permittivity as a pixel based plot. The pixel concentration is assumed to be proportional to the permittivity distribution of the two components inside the pixel in normalized scale. The permittivity distribution is also assumed to be proportional to material concentration inside the pixel. The image reconstruction algorithm used online in PTL300E is the so called Linear Back Projection Method. This is fast but approximate. There is a scope for using improved alternative algorithms (offline) like Iterative Image Reconstruction, Landweber and Tikhonov's method [13,14]. The twin plane ECT system used for vertical rig has 12 electrodes with driven axial guard electrodes. The data was captured at the rate of 100 frames/s and the electrodes were located on the outside of a 0.060 m diameter plexiglass pipe of length 0.51 m. The measurement electrode length is 0.0625 m and the separation between the sensor planes is 0.10 m. The flow analysis is done using offline software. The main features of the sensor are shown in Fig. 4.

For the pneumatic conveying flow rig at the Department of Chemical Engineering, University of Manchester, the measurements were obtained using a twin plane tomography system PTL 300 containing eight sensing electrodes at each plane and capable of collecting up to 100 images/s from both planes simultaneously. The schematic diagram of the sensor design of the above system is shown in Fig. 5.

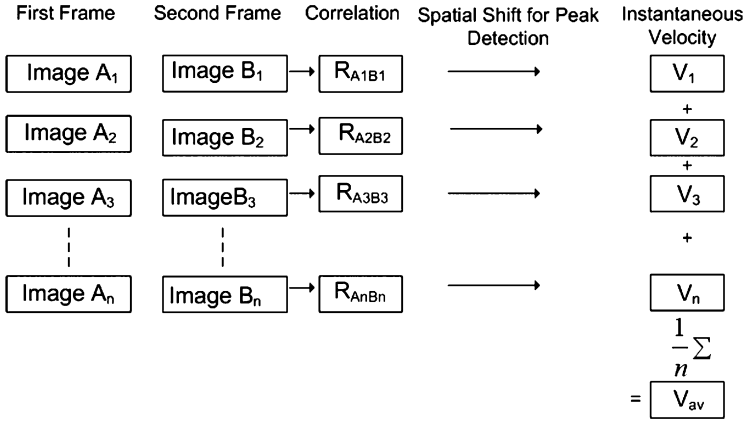

Fig. 3. Method of average velocity estimation based on [11].

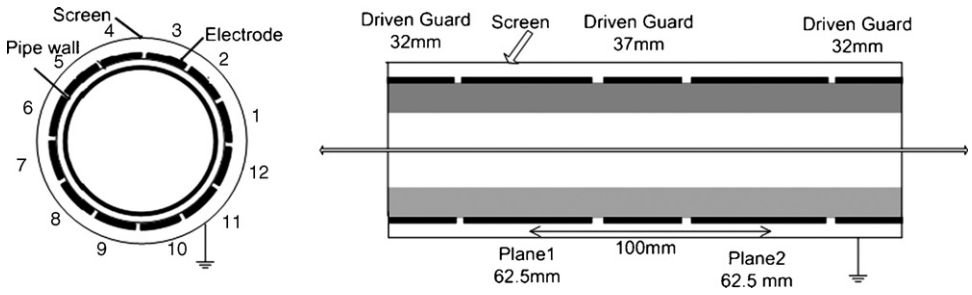

Fig. 4. Sensor design of 12-electrode PTL300E ECT system.

3.3. Laser Doppler Anemometer

Laser Doppler Anemometer (LDA) is a non-intrusive reliable and accurate method capable of measuring all three components of the flow velocity with high accuracy and high spatial resolution. It has a fast dynamic response and the ability to detect reversal flows for the particles, bubbles and droplets in single and as well as multiphase flow systems. There is a plethora of literatures about the use of LDA and Phase Doppler Anemometer (PDA) [15]. The two laser beams of equal intensity are focused to cross at the point of interest of the flow field. The fluid is seeded with minute tracer particles, which follow the motion of the fluid. When a particle passes through the control volume, light from each of the beams gets scattered and interfere. The scattered light of varying intensity fringe pattern is collected by a receiver lens and focused on a photo-detector. The detector signal is known as Doppler burst. The particle velocity U is related to the Doppler frequency shift f_D, intersection angle between the laser beam θ, and wavelength of the beam λ as

$$U = \frac{f_D \lambda}{2 \sin(\theta/2)} \tag{8}$$

4. Experimental set-up and measurement procedure

4.1. Flow in horizontal conveying

The pneumatic conveying rig used at the Department of Chemical Engineering, University of Manchester is shown in Fig. 6. The solids are supplied to the system from the bottom tank by means of a rotary feeder, and conveyed along a 7 m-long horizontal pipe section, a 3 m-long vertical section, and a 7 m-long return line. The solids are then discharged into the top tank. The capacity of tanks is 100 l each (approximately 55 kg of granular material). The internal diameter of the stainless steel pipe is 0.057 m.

The top tank is suspended on three load cells, which enable on-line weighing of the solids collected in the tank. This is used for the measurement of the mass flow rate of solids. It is calculated as an increase of the mass of the top tank divided by the time elapsed from the moment the gate valve between the top and bottom had been shut.

The granular material used in the experiment is polyamide chips of approximate dimensions 3 mm × 3 mm × 1 mm. The maximum feed rate for granular material used is approximately 900 kg/h. The air stream is introduced into the system by an 11 kW-blower and then it passes through a cooler to avoid rig overheating.

The air flow rate through the rig is kept independent from the solid flow rate by using a sonic nozzle. In this design, the gas flow rate is controlled only by the pressure upstream of the nozzle. This is set by adjusting a bleeding valve coupled with a pressure transducer. The air velocity (for an empty pipe) can be varied from 1.0 to 5.0 m/s by inserting three different sonic nozzles and varying the control pressure. The well defined dense-phase flow is typically obtained for the gas velocity within the region of 1.5–3.0 m/s and solids feed above 500 kg/h.

4.2. Flow in vertical conveying

A series of experiment has been done using a set-up of vertical pneumatic conveying rig in Telemark University College, Norway. The schematic diagram of the process is shown in Fig. 7. It consists of three main components as a silo with inserts for facilitating mass flow at the base, a vertical transport pipe and a

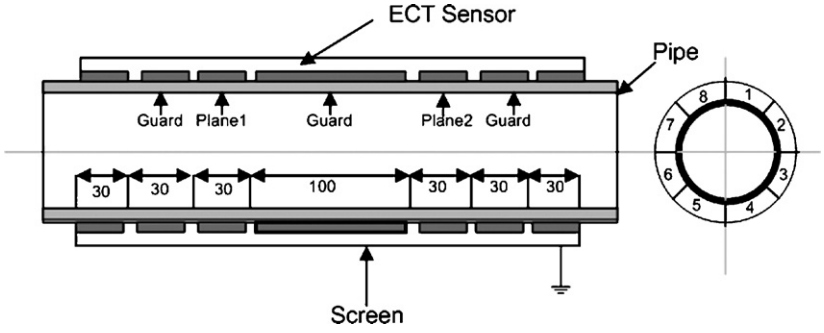

Fig. 5. Sensor design of eight-electrode PTL300 ECT system.

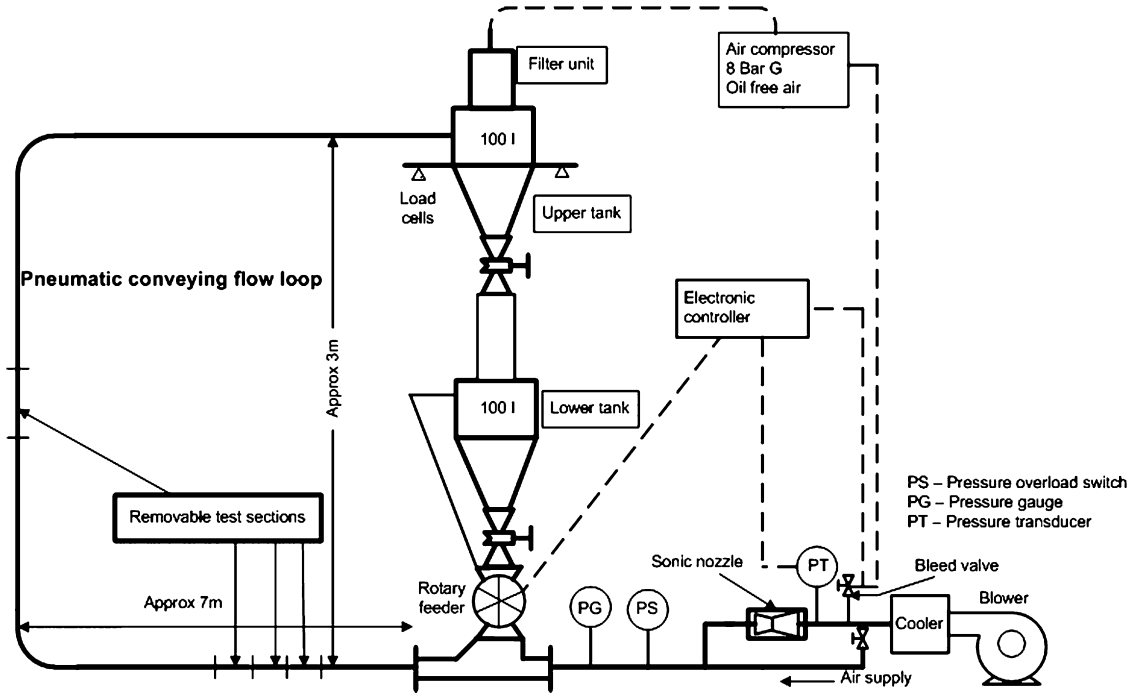

Fig. 6. A schematic diagram of the dense-phase pneumatic conveying rig used at the Department of Chemical Engineering, University of Manchester.

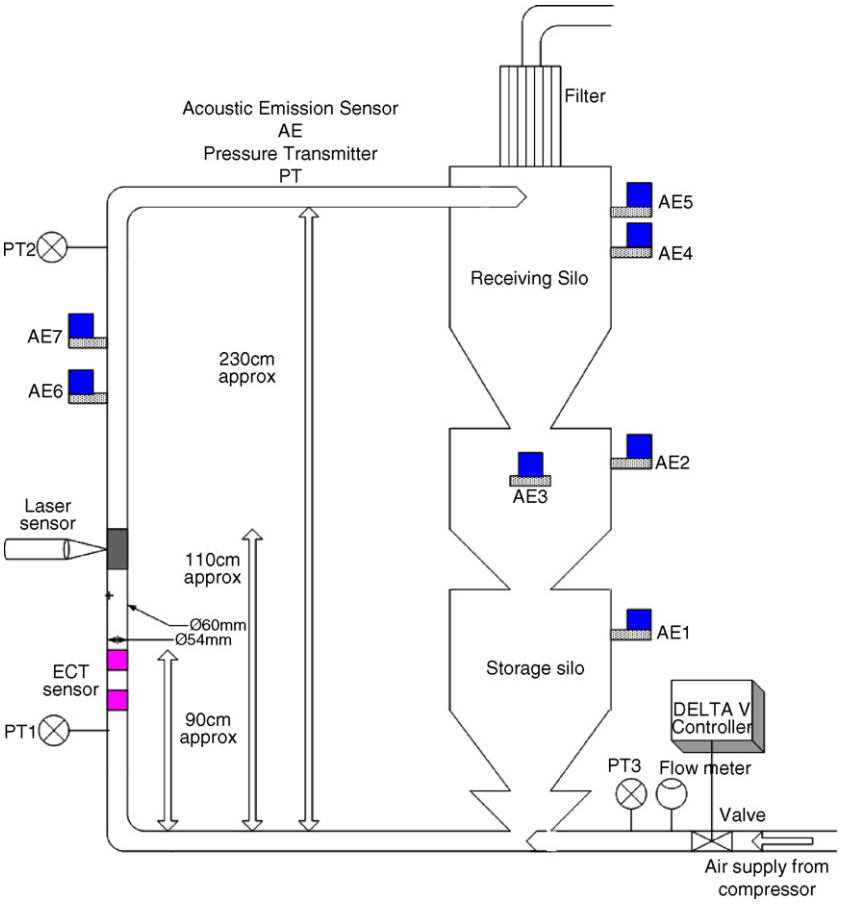

Fig. 7. A schematic diagram of vertical pneumatic conveying process used at Telemark University College, Norway.

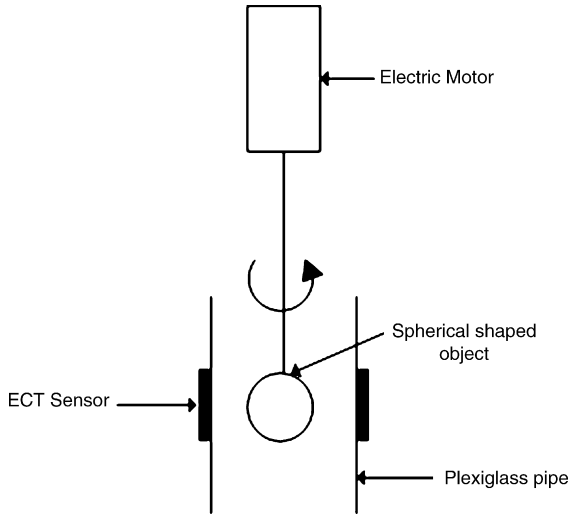

Fig. 8. Spherical dielectric object driven by a motor used in ECT based transverse velocity estimates.

receiving silo at the top. The material comes out of the silo into a feeding chamber with air supply. The length of the vertical rig is approximately 2.30 m and the outer diameter of the steel pipe is 0.060 m. Seven acoustic emission sensors are mounted at different positions on the vertical rig and silo wall shown in the diagram. The two acoustic emission sensors (AE6 and AE7), ECT sensors and LDA mounted on the vertical rig at different heights are used to monitor flow pattern. To measure the pressure and the air flow rate at the inlet position near the valve a pressure transmitter PT3 and a flowmeter are mounted. The airflow rate is controlled by a valve opening, which is connected to DELTA V automation system from Emerson Process Management. Two more pressure transducers PT1 and PT2 are also used to estimate the pressure drop in the rig and to calculate airflow rate in solid/gas phase at the position where the ECT system is mounted.

4.3. Rotational movement of an object in sensor plane

To facilitate easy verification of the method of estimating transverse velocity using pixel by pixel based correlation, a ball of high permeable material was placed in the ECT sensor head using LEGO modules. The LEGO modules were so assembled that a rotation of the high permeable ball was possible in the space within the ECT-sensor head.

A hollow spherical shaped object packed with zirconium oxide of high permittivity is rotated in a plane inside ECT sensor with different speed with the help of a motor by varying the voltage. The angular frequency of the rotation at different motor speed is measured with the help of a digital counter. The system consisting of the spherical dielectric object driven by a motor in the plane of capacitance sensors is shown in Fig. 8.

5. Results and discussion

5.1. Horizontal channel

The dense phase pneumatic conveying is realized by occurrence of plug or slug, which can be interpreted as wave phenomena. In horizontal conveying system it is formed when the gas velocity is reduced below the saltation velocity. The limitation of ECT system is that it measures average solid concentration of large control volume compared to particle size. So it is not possible to detect the trajectory of individual particle. The slug propagation velocity can be estimated using two axially separated sensor planes. The transverse component of slug is estimated using pixel by pixel correlation method. Figs. 9 and 10 show the transverse velocity vector plot of 99th frame and the magnitudes of the transverse velocity vectors at different pixel positions, respectively.

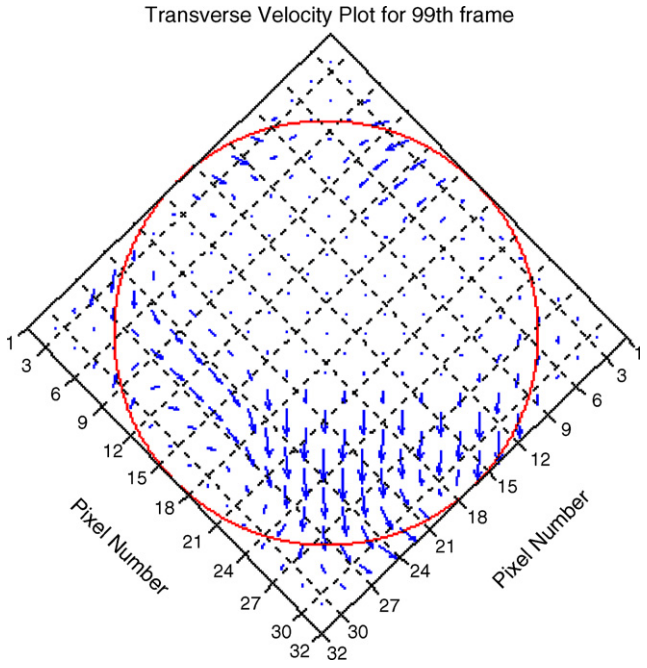

Fig. 9. Transverse velocity vector plot of 99th frame.

The vector plot is showing the movement of the material towards the bottom of the pipe. The transverse velocity component of the particles is probably caused by the picking up mechanism experienced by single particles to form a slug body.

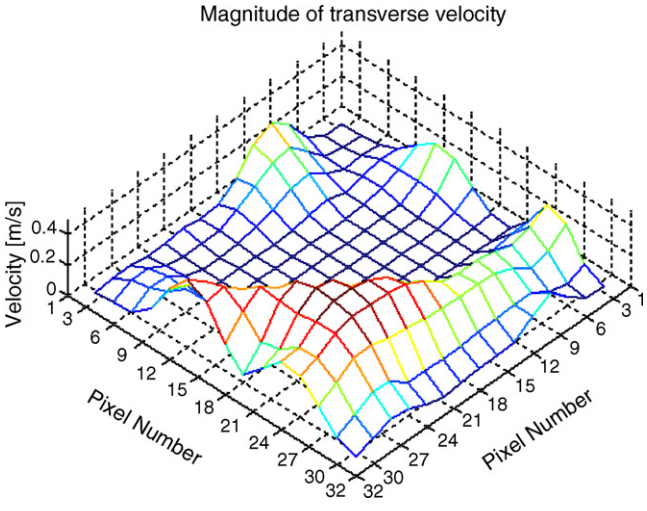

Fig. 10. Magnitude of transverse velocity.

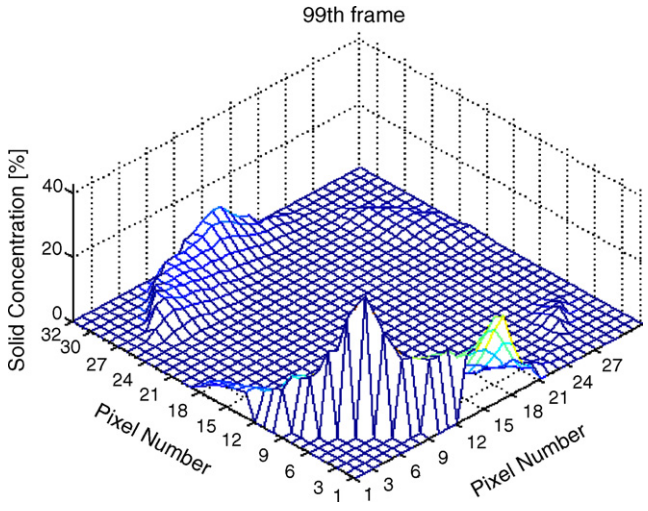

Fig. 11. Solid concentration of 99th frame.

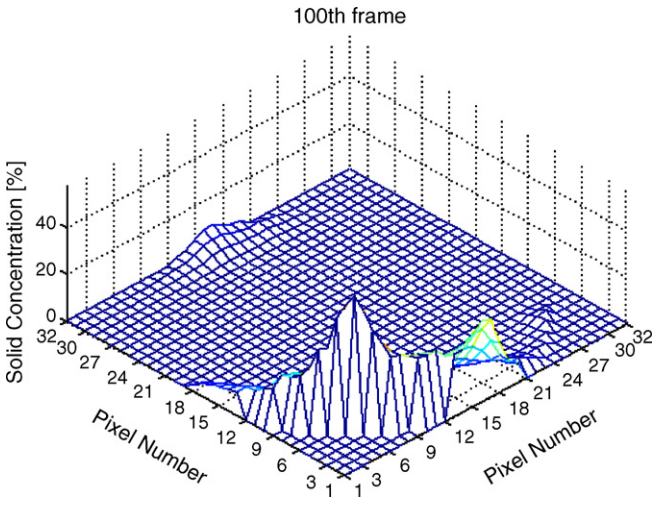

Fig. 12. Solid concentration of 100th frame.

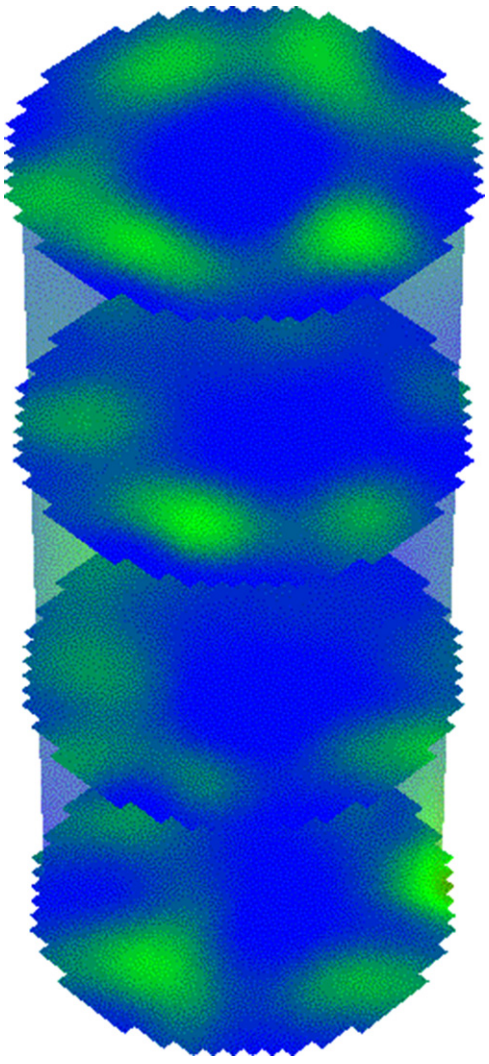

Fig. 14. Temporal variation of cross-sectional slices in three dimensions showing four slices.

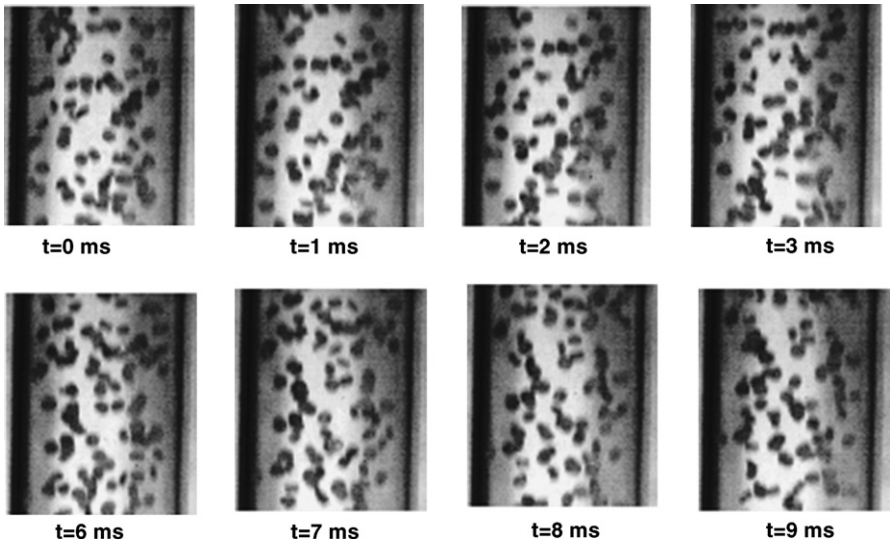

Fig. 13. Movement of the particulates inside the pipe captured by high speed camera at different instants.

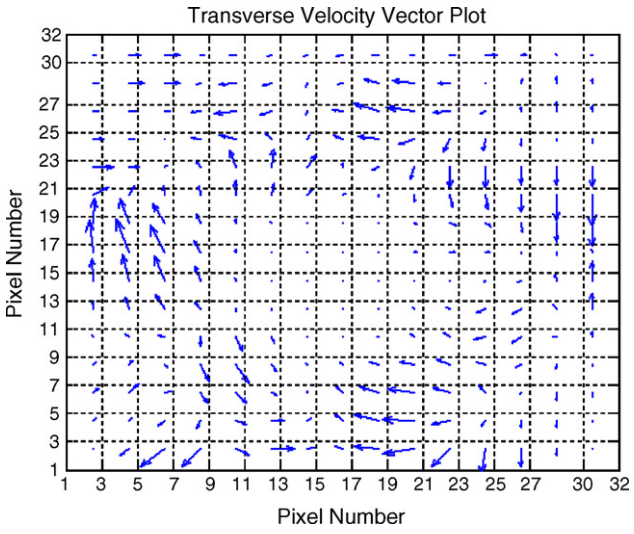

Fig. 15. Transverse velocity vector plot of 40th frame.

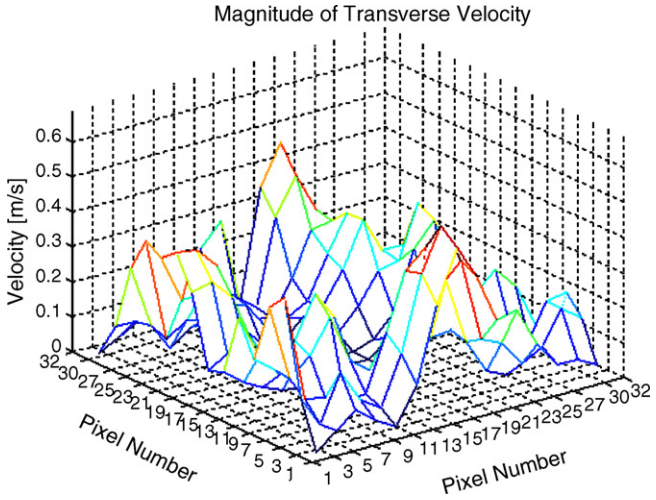

Fig. 16. Magnitude of transverse velocity of 40th frame.

In this mechanism, solids are picked up from settled layers and then conveyed axially to some distance [16,17]. The solid concentration as a function of pixel position for two consecutive frames (99 and 100) is plotted in Figs. 11 and 12.

5.2. Vertical channel

The materials used in the experiment is polyethylene pellets of average sieve size about 3.67×10^{-3} m and particle density 877 kg/m^3. The superficial velocity is varied between 9 m/s and approximately 13 m/s where the flow seemed to

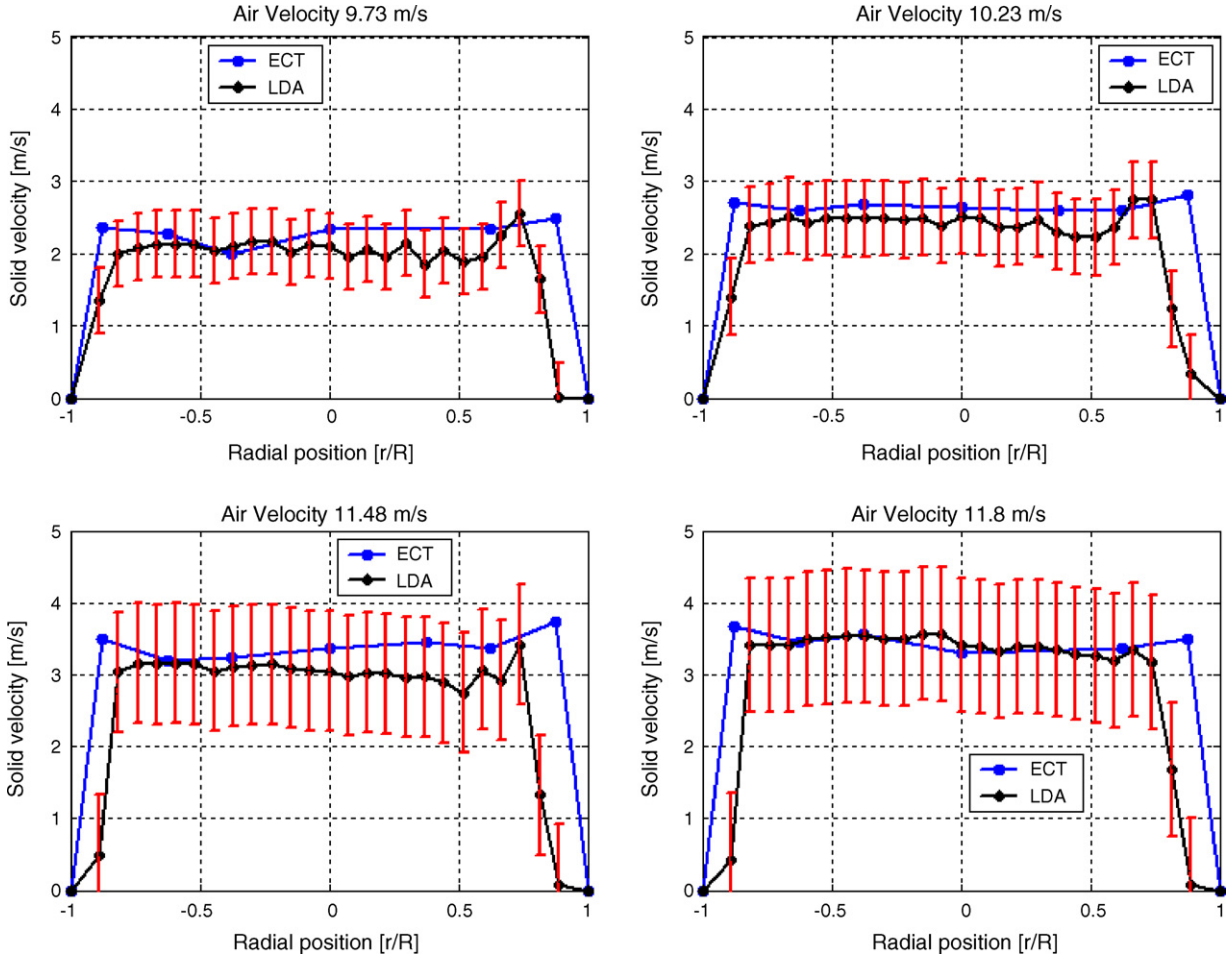

Fig. 17. Velocity profile over the cross-section by ECT and LDA method with error bar for different inlet air velocities.

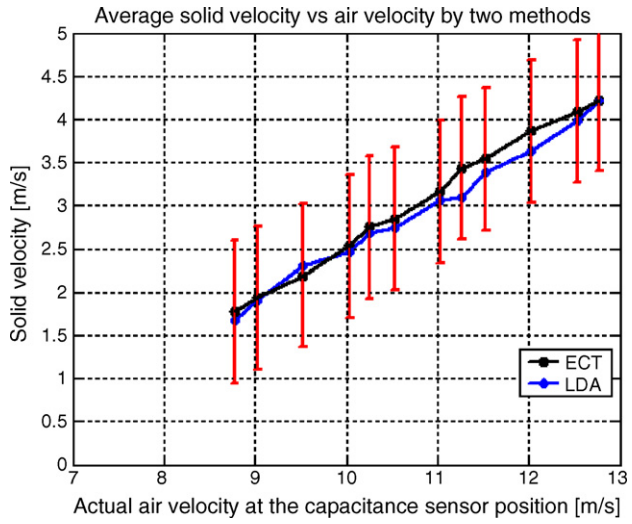

Fig. 18. Average axial solid velocities at different air velocities by ECT and LDA method over the whole cross-section.

be relatively steady. When the gas velocity is further lowered, flow becomes unsteady and the lift force is not sufficient for vertical conveying and as a result material falls down and ultimately it causes choking. This phenomenon observed in ECT based approach is also detected by high speed camera.

The pneumatic conveying process used shows that the flowmeter, which is mounted near the controlling valve is located at some distance from the feeder. So to understand the flow behaviour correctly at the position where ECT system is mounted the absolute pressure is measured at that position and thus air velocity is estimated considering the isothermal compression

$$PV = \text{constant} \tag{9}$$

where P is the pressure and V is the volumetric flow rate of air. Therefore the air velocity v_2 at ECT sensor position can be expressed as:

$$v_2 = \frac{P_1 v_1 A_1}{P_2 A_2} \tag{10}$$

where P_1 and P_2 are the pressures measured near the flowmeter and ECT system respectively. v_1 and A_1 are the superficial velocity and cross-sectional area at the flowmeter position respectively. A_2 is cross-sectional area of the pipe where ECT sensor is mounted. The gas transporting the solid flows through the suspended system and causes an increase of velocity over that for

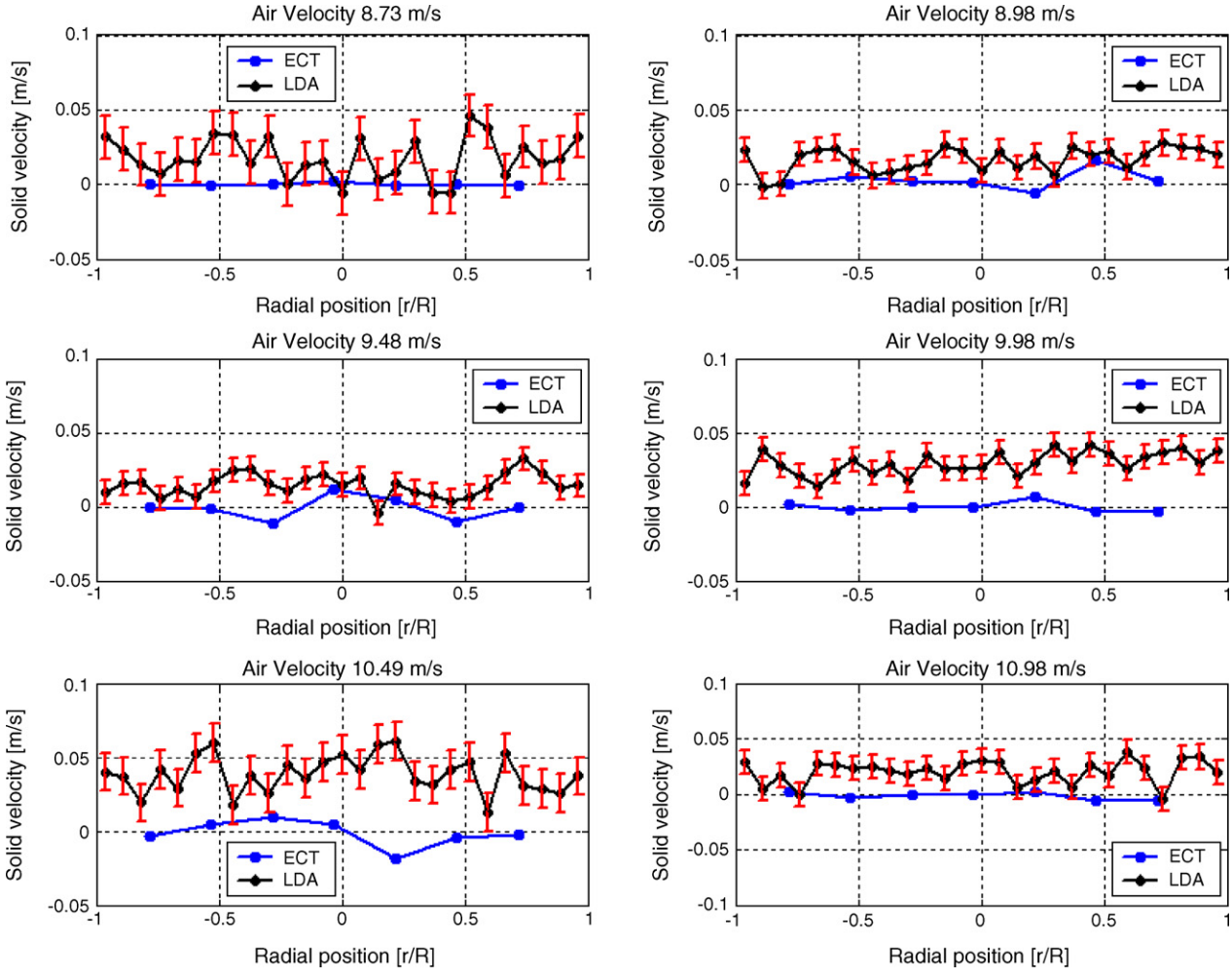

Fig. 19. Transverse component of solid velocities at different superficial velocities by ECT and LDA method.

an empty tube. So if the air velocity in an empty tube is v_g then the slip velocity can be expressed as [18]:

$$u_{slip} = \frac{v_g}{\varepsilon} - u_s \quad (11)$$

where u_s is the axial solid velocity and ε is the voidage. The instantaneous voidage is estimated from capacitive measurements.

The motions of the particles inside the pipe are observed by high-speed camera and still pictures at different time instants are shown in Fig. 13. It has been visualized that the particles travel in spiral fashion up in vertical conveying pipe with high concentration adjacent to the wall and less at the core region. This is also confirmed in a three-dimensional plot (Fig. 14) with equally spaced four cross-sectional slices obtained for a time duration of 0.1 s by using the Tomoflow Software. The electrostatic charge generation may be the key factor here for this type of pattern. In pneumatic conveying there is interparticle collision and also collision between the solid particles and pipe wall. At lower air flow rate when the dynamic equilibrium is established between drag force and the gravitational force, the electrostatic force due to charge generation acts as a dominant factor [19]. The electrostatic force responsible for particle trajectory is more significant [20] adjacent to the wall than the core and as a result particles concentrates more at the wall region than at the core.

5.2.1. Transverse velocity vector using proposed pixel based technique

The proposed pixel based correlation technique was used to find the transverse velocity at various inlet airflow rates. Fig. 15 shows that the transverse velocity vector plot over the cross-section for the 40th frame and the magnitude of transverse velocity for the same frame is plotted in Fig. 16.

5.2.2. ECT-based estimation of velocity versus LDA measurements

Both the axial and transverse velocity estimation obtained by ECT system is validated using established LDA method.

- Axial velocity

  The axial velocity profiles over the cross-section at different inlet air velocities are estimated using both ECT and LDA. Fig. 17 shows the comparison of solid velocity distribution profiles at different inlet air velocities with error bar of LDA measurement. The results show that ECT measurement data is well within the range of error bound of LDA estimation. The error bar shows two standard deviation units in length. The average axial solid velocities over the cross-section estimated at different air velocities by both the methods are shown in Fig. 18.
- Transverse velocity

  The transverse component of solid velocity using the proposed algorithm is compared at different airflow rates with the estimated velocity by LDA method. Fig. 19 shows that for low superficial air velocity as the solid concentration is more typically in the range of 4–5% the measured velocity by pixel based correlation is well within the range of LDA measurements. But at higher air velocity as the solid concentration becomes low, the pixel based correlation estimate deviates from the LDA measurements. The main source of estimation of pixel based correlation algorithm is reconstructed image obtained from capacitance measurements and at lower material concentration there is more probability of error introduced due to low pixel concentration. Therefore at higher air velocity, when the solid concentration is less, there is large discrepancy in transverse solid velocity measurement by this method from the LDA measurement. The fundamental principles of velocity measurement by both methods are different and they are neither measured simultaneously nor at the same position. Fig. 20 shows the standard deviation of the velocity distribution estimated using LDA measurements at different air velocities.

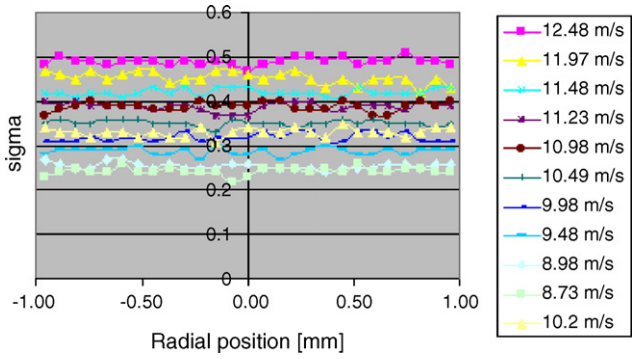

Fig. 20. Standard deviation of transverse component of velocities using LDA.

5.3. Rotational movement of an object in sensor plane

The proposed pixel based correlation technique was implemented to trace the path of the spherical object rotated in sensor plane at different speeds. To verify the proposed correlation technique the obtained transverse velocity is plotted in Fig. 21 as a function of motor voltage. The plot shows clearly two clusters A and B. In the region A the function is fairly lin-

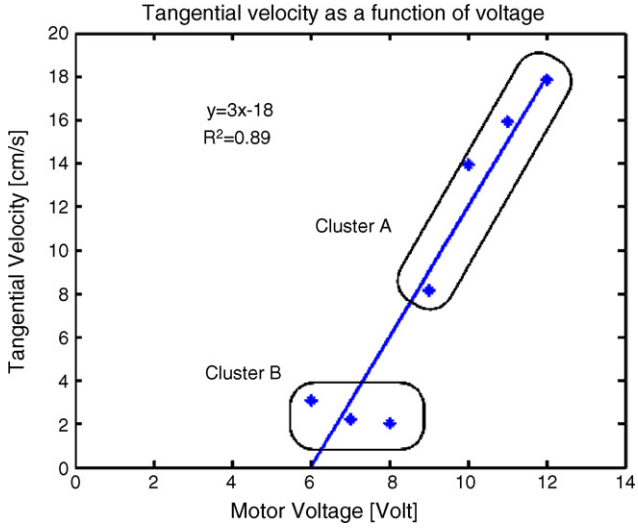

Fig. 21. Variation of correlated velocity with motor voltage.

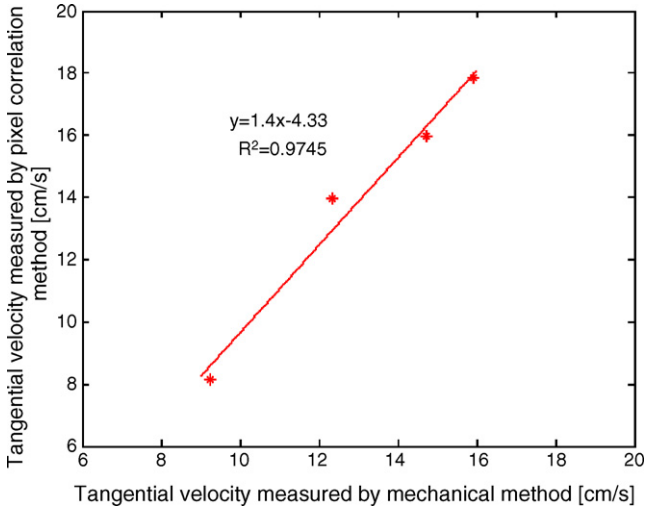

Fig. 22. Comparison of transverse velocities obtained by pixel based correlation method with tangential velocities estimated using maximum density pixels.

ear, whereas in region B, there is considerable deviation due to non-circular and vibratory motions. The rotational velocity is estimated theoretically based on the equation relating tangential velocity v_i at the ith pixel at radius r_i with its angular velocity ω_i using:

$$v_i = r_i \omega_i. \tag{12}$$

The pixel showing the maximum density is used to calculate the tangential velocity $v_{i_{\max}}$. The correlation based estimated transverse velocities are then compared with theoretically calculated velocities shown in Fig. 22. Fig. 23 shows the movement of the object in the cross-section of the pipe for the cluster A. Fig. 24 displays direction and magnitude of velocity vectors as arrows emanating from the origin. The radius of each concentric circle shows the magnitude and angle shows the direction. The magnitude and the direction of the velocity vectors obtained by pixel-based technique shown in the figure confirm the circular motion of the object.

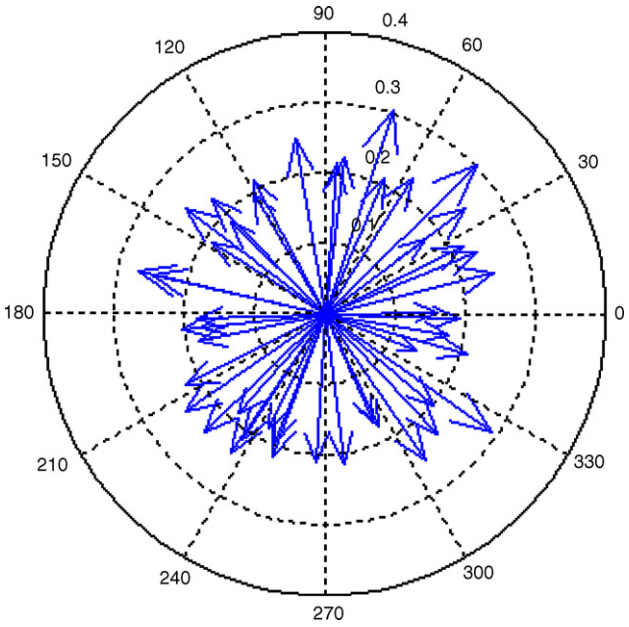

Fig. 24. Compass plot of the motion of the object.

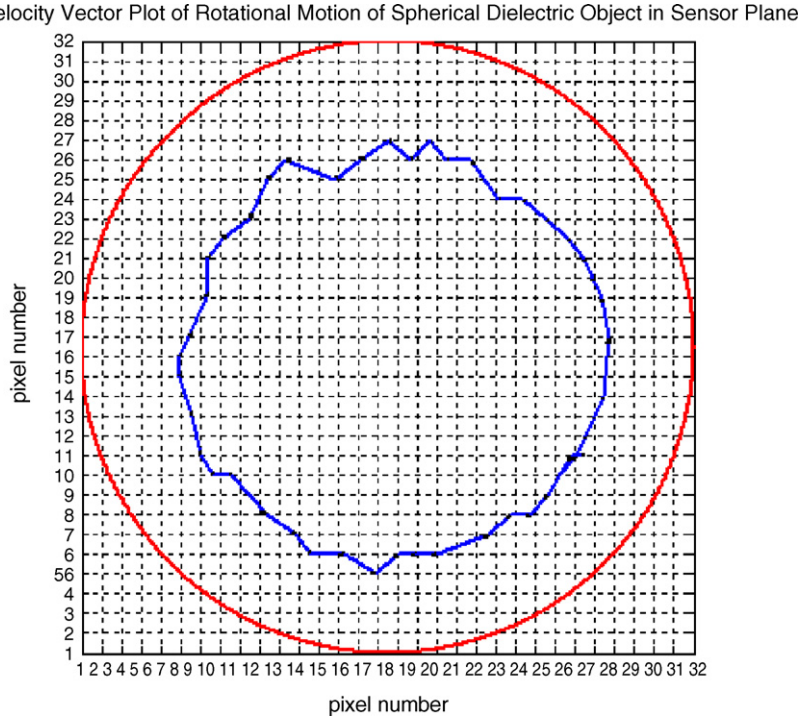

Fig. 23. Velocity vector plot of the object in cross-sectional area for cluster A.

6. Conclusions and future work

In pixel by pixel correlation technique when concentration values of all the pixels in a frame are correlated with all pixels of next frame in the same plane, we get the information of only one velocity vector for a pair of frame from the projected distance between the chosen pixel pairs. If there is only one object in the cross-section, that means a high concentration gradient, then with this method we clearly get the trace of the path of the object. But in three dimensional multiphase flows there is material distribution all over the pipe cross-section and to understand the trajectory of the materials in transverse direction it is important to get the full picture of velocity vectors in two dimensional field. So an improved method is further proposed considering an interrogation window by grouping the pixels. The conventional PIV algorithm [21] evaluates a cross-correlation between two interrogation windows centred at particular position and coming from two different frames. A similar technique is developed using ECT image. Single pixel resolution correlation algorithm [22] in PIV calculates spatial correlation between single pixels of the first image with all the pixels of the second image in the interrogation window for a set of double frames. Similar technique is applied in tomographic scenario considering a set of double frames and thus performing instantaneous correlation and the averaged velocity function. The nonlinear operation of peak detection leads to erroneous velocity measurements when the signal to noise ratio is low. When the concentration is low, i.e. the pixel value is low, there may not be adequate signal to obtain valid velocity measurements from the instantaneous correlation function. This is clearly observed when transverse velocity distribution profile obtained by ECT is compared with LDA method at low image concentration. Furthermore the two consecutive image frames separated by known time delay Δt used for instantaneous cross-correlation are assumed to represent a single realization of a statistically stationary process. But in practice as there is limitation in frame rate in ECT system and for transient multiphase flows, implying one of the main drawbacks of the technique developed. Some of these issues have been addressed in the context of ERT-measurements in Wang et al. [23].

Acknowledgements

This work is funded by the Research Council of Norway. Many thanks are due Mr. Talleiv Skredtvedt of Telemark University College, for the silo design and for the help with all the experimental set-ups needed for this study.

References

[1] A. Plaskowski, M.S. Beck, R. Thorn, T. Dyakowski, Imaging Industrial Flows: Applications of Electrical Process Tomography, Institute of Physics Publishing, Bristol, UK, Philadelphia, 1995.

[2] R.A. Williams, M.S. Beck (Eds.), Process Tomography: Principles, Techniques and Applications, Butterworth-Heinemann, Oxford, 1995.

[3] V. Mosorov, D. Sankowski, L. Mazurkiewicz, T. Dyakowski, The 'best-correlated pixels' method for solid mass flow measurements using electrical capacitance tomography, Meas. Sci. Technol. 13 (2002) 1810–1814.

[4] Y. Zhang, J. Yao, C.H. Wang, Electrical capacitance tomography measurements on inclined conveying pipes, in: Proceedings of the Fourth World Congress on Industrial Process Tomography, Aizu, Japan, 2005, pp. 404–409.

[5] G.T. Bolton, C.W. Hooper, R. Mann, E.H. Stitt, Flow distribution and velocity measurement in radial flow fixed bed reactor using electrical resistance tomography, Chem. Eng. Sci. 59 (2004) 1989–1997.

[6] M.L. Jakobsen, W.J. Easson, C.A. Greated, D.H. Glass, Particle image velocimetry: simultaneous two-phase flow measurements, Meas. Sci. Technol. 7 (1996) 1270–1280.

[7] M.S. Beck, A. Plaskowski, Cross-correlation Flowmeters—Their Design and Application, Adam Hilger, Bristol, 1987.

[8] U. Datta, V. Mathiesen, S. Mylvaganam, Tomometric approach using multi sensor data fusion in particle segregation studies, in: Proceedings of the Third World Congress on Industrial Process Tomography, Banff, Canada, 2003, pp. 510–515.

[9] E.O. Etuke, R.T. Bonnecaze, Measurement of angular velocities using electrical impedance tomography, Flow Meas. Instrum. 9 (3) (1998) 159–169.

[10] U. Datta, S. Mylvaganam, T. Dyakowski, Estimating transverse velocity components of slug flow using pixel by pixel correlation method via ECT, in: Proceedings of the Fourth World Congress on Industrial Process Tomography, Aizu, Japan, 2005, pp. 374–379.

[11] C.D. Meinhart, S.T. Wereley, J.G. Santiago, A PIV algorithm for estimating time-averaged velocity fields, J. Fluids Eng. 122 (2000) 285–289.

[12] J. Westerweel, Efficient detection of spurious vectors in particle image velocimetry data, Exp. Fluids 16 (1994) 236–247.

[13] PTL300E-TP-G ECT system operational manual, Process Tomography LTD, 2003.

[14] W.Q. Yang, L. Peng, Image reconstruction algorithms for electrical capacitance tomography, Meas. Sci. Technol. 14 (2003) R1–R13.

[15] V. Mathiesen, T. Solberg, Laser Doppler anemometry measurements of dilute phase pneumatic transport in vertical filter, in: Proceedings of the Fourth International Particle Technology Forum, AICHE Annual Meeting, Los Angeles, 2000.

[16] A.J. Jaworski, T. Dyakowski, Tomographic measurements of solid mass flow in dense pneumatic conveying. What do we need to know about the flow physics? in: Proceedings of the Second World Congress on Industrial Process Tomography, Hannover, Germany, 2001, pp. 353–361.

[17] A.J. Jaworski, T. Dyakowski, Application of electrical capacitance tomography for measurement of gas-solid flow characteristics in a pneumatic conveying system Meas. Sci. Technol. 12 (2001) 1109–1119.

[18] G.E. Klinzing, R.D. Marcus, F. Rizk, L.S. Leung, Pneumatic Conveying of Solids—A Theoretical and Practical Approach, 2nd ed., Chapman and Hall, UK, 1997.

[19] J. Yao, Y. Zhang, C.H. Wang, S. Matsusaka, H. Masuda, Electrostatics of the granular flow in pneumatic conveying system, Ind. Eng. Chem. Res. 43 (2004) 7181–7199.

[20] C.P. Yu, Precipitation of unipolarly charged particles in cylindrical and spherical vessels, J. Aerosol. Sci. 8 (1977) 237–241.

[21] K. Jambunathan, X.Y. Ju, B.N. Dobbins, S. Ashforth-Frost, An improved cross-correlation technique for particle image velocimetry, Meas. Sci. Technol. 6 (1995) 507–514.

[22] F. Billy, L. David, G. Pineau, Single pixel resolution correlation applied to unsteady flow measurements, Meas. Sci. Technol. 15 (2004) 1039–1045.

[23] M. Wang, W. Yin, Measurements of the concentration and velocity distribution in miscible liquid mixing using electrical resistance tomography Part A, Trans. IChemE 79 (2001) 883–886.